

Performance Testing of a Solar Thermal Fruit Dryer – A Case Study to Reduce Food Waste in Mozambique

Viktor Döhlen¹, Gustaf Bengtsson¹, Randi Phinney² and L. Ricardo Bernardo¹

1 Department of Architecture and Built Environment, Division of Energy and Building Design, Lund University, Lund, Sweden

2 Department of Food Technology, Engineering and Nutrition, Lund University, Lund, Sweden

Abstract

The purpose of this project is to investigate an innovative technology for sustainable preservation of juicy fruits in developing countries with the aid of simple solar thermal drying technology. Approximately five million tonnes of citrus fruit produced in Mozambique is annually wasted (FAOSTAT, 2015). A large solar energy potential and large fruit spoilage in Mozambique present the opportunity to implement a simple method for fruit preservation, combining solar thermal drying with a semipermeable membrane bag containing fruit juice. A small-scale indirect passive solar air dryer for drying the membrane bags was constructed and evaluated in terms of drying flux as a function of temperature, relative humidity and air flow rate. Measurements were initially carried out in the laboratory and later complemented with a field study in Mozambique. The dryer achieved a temperature interval that was required for high quality fruit drying and lowered the relative humidity. However, it was further found that air flow passing over the bags acted as an important parameter in the drying meaning that an increased air flow rate increased the drying flux to a larger extent than first assumed. The findings provide insight on the drying process and on how to improve the design of the solar air dryer.

Keywords: *Solar Thermal, Indirect Solar Dryer, Semipermeable Membrane, Fruit Drying, Food Waste, Development Project.*

1. Introduction

Fruit is abundant in Mozambique, both farmed and wild, yet much of it spoils post-harvest or is never even picked due to the large amounts that ripen during a short harvesting season. Long-term storage possibilities are uncommon since industrial preservation technologies require large amounts of clean water and power – something limited in rural Mozambique (Phinney et al., 2015). One contributing solution to this problem could be the combination of solar thermal dryers with a newly developed breathable membrane bag to facilitate drying of fruit juices and purées in Mozambique. This means that juicy fruits, such as oranges and tangerines, that are difficult to dehydrate using traditional open-air sun drying, could also be dried. Preservation with the membrane bags only requires suitable ambient conditions since the drying process is largely driven by a lower relative humidity in the air surrounding the bags. The objective of using a solar dryer is to protect the bags from external disturbances and supply the process with more heat than the ambient conditions can provide (Ekechukwu and Norton, 1997), increasing the temperature and thus decreasing the relative humidity. This technological combination results in a system independent of external electric power and large amounts of clean water and thus is more suitable for rural areas lacking developed infrastructure (Ekechukwu and Norton, 1997; Otte, 2014). To ensure fruit preservation of high quality, the drying has to be performed using an adequate temperature interval. The aim of the research is to construct a solar dryer for enhancing the drying of the membrane bags and to understand the underlying mechanisms behind this drying process so that future dryers coupled with membrane bags can be properly optimised.

2. Theory

2.1. Theory behind the technique

Drying is the process of removing water from a product. In this study, drying of a liquid product was achieved using a membrane bag and a technique called Solar Assisted Pervaporation (SAP) (Phinney et al., 2015). Pervaporation is a process in which a non-porous semi-permeable membrane is used to separate one or more chemical species from one or more other chemical species. The species that diffuses through the membrane also has an affinity for it, or in other words the species “wets” the membrane (Néel, 1991). In the case of Solar Assisted Pervaporation, the membrane is hydrophilic and water molecules are able to diffuse through the void spaces of the polymer molecules that make up the membrane. The membrane acts as a selective barrier, letting water vapour molecules through while keeping the liquid water and other nutrients inside the bag (Phinney et al., 2015).

The SAP process is driven by a water vapour partial pressure difference across the membrane, where the partial pressure is a function of temperature (i.e. it increases with increasing temperature) (Pervatech BV, 2014). Inside the bag, the initial water vapour partial pressure is close to the saturation pressure whereas outside the bag, the partial pressure corresponds to the relative humidity (RH) of the surrounding air. If the RH of the surrounding air is less than 100%, a water vapour partial pressure gradient across the membrane will exist and drying will proceed (Saravacos and Kostaropoulos, 2002). Solar energy enhances the process by supplying the latent heat of evaporation and reducing the RH of the air surrounding the bag. As the second law of thermodynamics states: diffusion of a species will occur as long as a difference in saturation exists, striving for an equilibrium (Cengel and Boles, 2011).

The amount of mass transferred from the bag to the surrounding air over time, \dot{m} ($\text{kg}\cdot\text{s}^{-1}$), due to diffusion through the membrane is a function of the overall mass transfer coefficient, K ($\text{kg}\cdot\text{m}^{-2}\cdot\text{s}^{-1}\cdot\text{Pa}^{-1}$), the total membrane surface area, A_s (m^2), and the difference in water vapour partial pressure (with units of Pa) on the inside ($p_{w,sat @ T_1}$) and outside ($p_{w,\infty @ T_2}$) of the bag, where T_1 is the surface temperature and T_2 is the surrounding air temperature in degrees Celsius (Bergman et al, 2007). The heat and mass transfer phenomena taking place can be compared to the case of an open dish with water where in both cases, water vapour is assumed to be an ideal gas. Since RH is equal to the ratio between $p_{w,\infty}$ and $p_{w,sat}$ at a given temperature, the RH on the inside of the bag is 100% and in the surrounding air is $p_{w,\infty @ T_2}$ divided by $p_{w,sat @ T_2}$ and then multiplied by 100 (note: $p_{w,sat @ T_1}$ and $p_{w,sat @ T_2}$ are only equal if T_1 and T_2 are equal, which is not always the case). The main differences between our case and that of an open water dish is a resistance provided by the polymer membrane (which reduces K), and that the open dish has only one drying surface whereas the bag has two (which means A_s is twice as large for a bag of the same length and width). Equation 1 shows how the mass transfer rate is affected by the mass transfer coefficient, surface area and water vapour partial pressure. Mass transfer flux is defined as \dot{m}/A_s and is the quantity referred to in the remainder of the paper.

$$\dot{m} = K \times A_s \times (p_{w,sat @ T_1} - p_{w,\infty @ T_2}) \quad (\text{eq. 1})$$

2.2. Temperature as a function of flow rate

As relative humidity is a function of temperature, the speed of water removal in the dryer is dependent on temperature. In addition, the quality of the end-product (e.g. related to vitamin losses) requires a set temperature interval. The small-scale solar thermal dryer's gained energy over time, absorbed by the collector, can be calculated by measuring global irradiance, G ($\text{W}\cdot\text{m}^{-2}$), for an angle of incidence normal to the glass of the dryer, on the collector area, A_c (m^2). A thermal efficiency ($\eta_{thermal}$) is introduced to include the heat losses, the material properties and the optical losses into account. This efficiency only serves as a rough estimate on how much energy is put to use in the dryer as hot air. An equation for the power transfer from the sun to the air can be written as:

$$\dot{Q}_{gain} = G \times \eta_{thermal} \times A_c \quad (\text{eq. 2})$$

The amount of useful energy over time can also be calculated by looking at the collector as a control volume with a temperature difference over the absorber area.

$$\dot{Q}_{gain} = A_{cs} \times v \times \rho \times c_p (T_{out} - T_{in}) \quad (\text{eq. 3})$$

where A_{cs} (m^2) is the cross section area, v is the flow rate normal to the cross section, ρ ($\text{kg}\cdot\text{m}^{-3}$) is the fluid's density, C_p ($\text{J}\cdot\text{kg}^{-1}\cdot\text{K}^{-1}$) is the specific heat capacity at a constant pressure, T_{in} is the temperature of the air entering the collector and T_{out} is the outlet temperature of the collector. The velocity varies spatially due to the flow profile in the collector. Therefore, a mean has to be calculated, based on reference measurement points over the cross section width, from measurement standard SS-EN-1505 (Johansson and Svensson, 1998). Combining equations 2 and 3 and isolating T_{out} :

$$T_{out} = T_{in} + \frac{G \times \eta_{thermal} \times A_c}{A_{cs} \times v \times \rho \times c_p} \quad (\text{eq. 4})$$

Which results in the outlet temperature as a function of the flow rate in the dryer. The flow rate can be adjusted by regulated the air outlet opening size.

3. Method

3.1. Construction of the solar dryer

A prototype small-scale solar thermal dryer was constructed in Lund before the field study was conducted. The result is presented in Figure 1 with a schematic illustration of the basic technique of natural ventilation, along with dimensions. The implementation of the solar dryer would take place in a developing country, something the design of the dryer had to account for. This means that complexity had to be minimized and user friendliness maximized. Furthermore, the design of the solar dryer had to meet the posed criteria of temperature and size. A temperature interval defined by a lower temperature of 50 °C to prevent microbial growth and a higher limit of 65 °C to minimise degradation of ascorbic acid was set as desirable (Rab et al, 2015). The size, presented in Table 1, is limited to a small-scale solar thermal dryer, possible to transport on conventional flights.

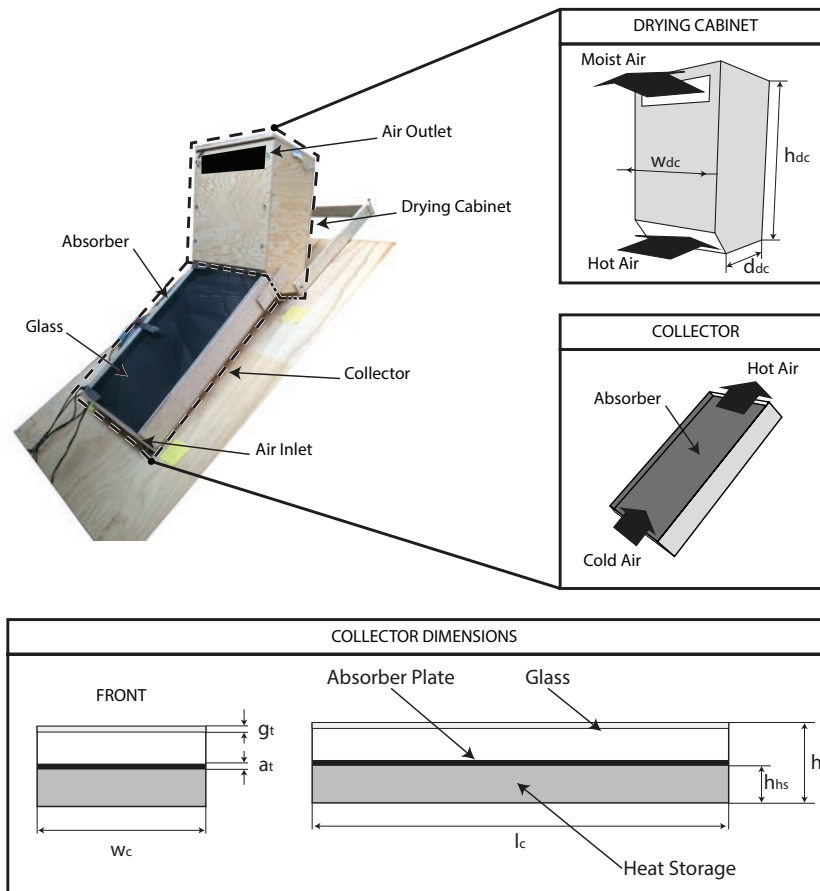


Fig. 1: Picture of the constructed solar dryer, with a schematic illustration of the collector, to illustrate the dimensions of the dryer.

Tab. 1: Table of the small-scale solar thermal dryer's dimensions.

Collector Parts	Dimensions
Length, l_c	0.700 m
Outer width, w_o	0.424 m
Width absorber plate, w_a	0.376 m
Height collector, h_c	0.082 m
Distance absorber-glass, d_{a-g}	0.035 m
Height heat storage, h_{hs}	0.035 m
Thickness absorber, a_t	0.012 m
Thickness glass, g_t	0.003 m
Drying Cabinet Parts	
Height, h_{dc}	0.500 m
Width, w_{dc}	0.400 m
Depth, d_{dc}	0.200 m

3.2. Measurement setup

The semi-permeable bag consists of a breathable polymer that is permeable to water vapour but not liquid water, as stated in the theory section. This means that during drying, all of the liquid water is contained in the bag, while water vapour is able to diffuse through the membrane and then escape to the surroundings. For a more detailed description of the procedure and SAP technique, please refer to Phinney et al., 2015. Previous

testing from the mentioned study with a bag prototype suggested a constant drying flux is achieved at the beginning of drying if the product to be dried is very watery (e.g. fruit juice). Wind speed was not found to play a crucial role in previous testing due to the nature of the equipment used where the air flow was able to pass horizontally over both sides of the bag. Figure 2 presents a picture of the membrane bags filled with water. The height of the bags are 19 cm, and width of 7.5 cm. Thickness varied depending on different amount of water in the bags, between 2 to 4 cm.

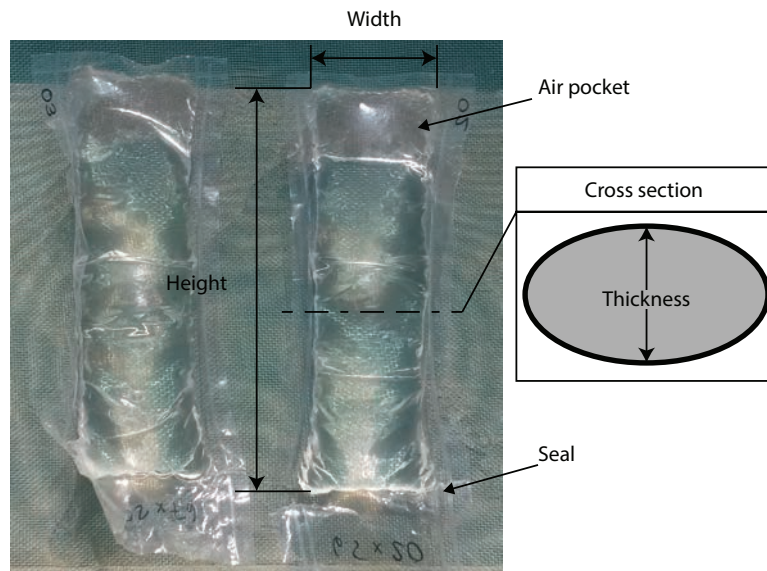


Fig. 2: Picture of the transparent membrane bags filled with water that were dried on-site in Mozambique..

The measurement equipment was setup to gather data on temperatures in the collector and drying cabinet, the relative humidity in the ambient environment and inside the drying cabinet, mass loss, wind speed and irradiance. The equipment was installed at the following points illustrated in Figure 3. The measurement points used in this article are points number 3, 9 and mass loss found by the hand scale represented at point 12.

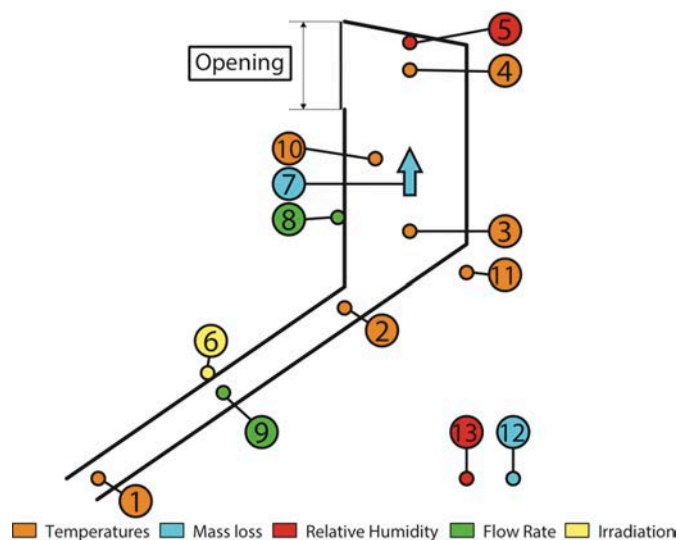


Fig. 3: A schematic figure of the measurement setup for the field testing.

3.3. Performance testing

The performance tests consisted of investigating the drying flux (\dot{m}/A_s) of the bags in the dryer over the course of a day. The separate tests are referred to as Run 1 to 6. The test runs begun by weighing the bags before they were inserted in the drying cabinet and ended by weighing after removal from the same space, in order to identify a linear representation of the mass loss over time per unit surface area. All membrane bags used were rectangular with dimensions of 0.19 ± 0.005 m times 0.075 ± 0.005 m. The bags consisted of two sides, resulting in a total active surface area of 0.0266 ± 0.0025 m². The bags were filled with water, not fruit juice, since the aim of the project was to investigate how the conditions in the dryer affected the drying flux, and water was deemed easier to handle than fruit juice. The drying process of water in the bags is similar to the first stage of drying juice, otherwise known as the constant rate or constant flux period, when the water at the surface of the juice is still plentiful and internal mass transport is not yet dominating (Phinney et al., 2015).

The test aimed to reach a stable input of solar energy, by rotating the dryer along the solar azimuth angle every hour and regulating the temperature and air-flow in the dryer by adjusting the opening of the air outlet. These parameter changes are presented in Table 2. The resulting drying fluxes were later analysed to identify how drying flux could relate to temperature and air flow rate regulation in the dryer. The drying flux of the bags was later compared to a reference bag placed out in the open beside the dryer to evaluate the relative speed.

Tab. 2: Table representing the approximated amount of time each air outlet opening was used during Runs 1-6.

Opening /%	Run 1	Run 2	Run 3	Run 4	Run 5	Run 6
0	2 h					
16	2 h	1 h		3.5 h		
33	1 h	2 h		2 h		
50		2.5 h	4 h		5.25 h	3.5 h
100			3 h			2.5 h

3.4. Design changes

The dryer's design was examined after Runs 1, 2 and 3 and then the drying cabinet's volume was decreased by reducing the depth to 7 cm instead of 20 cm to increase the flow rate through the drying cabinet, illustrated in Figure 4. The hypothesis was that an increased flow rate passing the bags would increase the drying flux. The bag was hung vertically to fit in the smaller space, leading to a change in the characteristic length of flow passing over the bag.

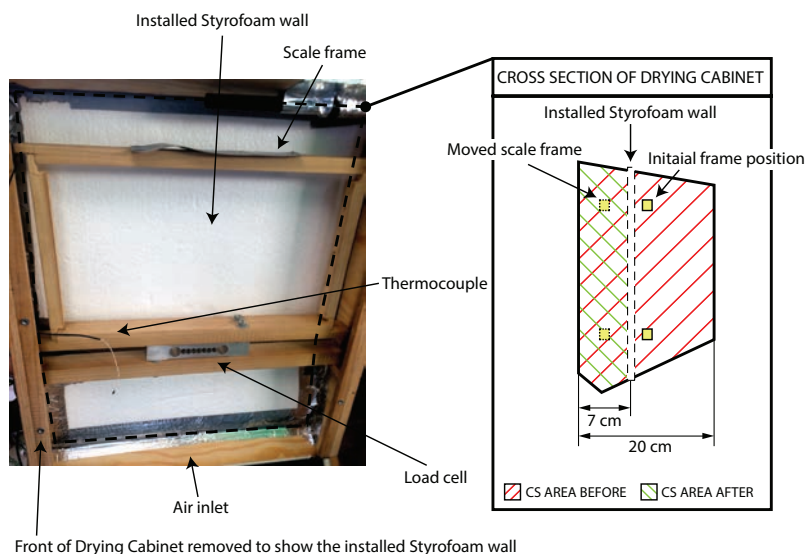


Fig. 4: Illustration of how the design change decreased the cross-sectional area of the drying.

4. Results

Table 3 presents measurement results of the drying flux of the bags as a function of the mean temperature (measurement point 3) in the drying cabinet and the air flow rate passing over the bags. Runs 1 to 6 are shown and compared to the reference bag dried at outdoor ambient conditions. Results for the drying flux are averaged over the course of a day. The results are presented ranging from the lowest to highest percentage of air outlet opening, where the first three runs represent the original design and Runs 4-6 represent the implemented design change with a smaller cross-sectional area. The air flow velocity is not corresponding entirely as it is higher for run 5 than run 6, which can be due to ambient weather conditions. Another anomaly is the drying flux for Run 2, which is not following the trend, since three bags were present in the dryer as opposed to the other runs where only one bag was present. Figure 5 and Figure 6 present the results in a graphical manner, where the values for the drying flux is plotted over air flow velocity. A linear approximation is introduced to illustrate the relationship between these variables. To be noted, the drying flux inside the dryer system never exceeded that of the reference bag, as presented in Table 3, but the run with the highest air flow rate reached approximately the same value.

Tab. 3: The results are presented ranging from the lowest to highest percentage of air outlet opening.

Test	Opening /%	Time	Drying Flux / $\text{g}\cdot\text{m}^{-2}\cdot\text{h}^{-1}$	Temperature / $^{\circ}\text{C}$	Air Flow Velocity / $\text{m}\cdot\text{s}^{-1}$
Run 1	16 & 0	10:38-15:39	182.3	45.8	0.0190
Run 2	33 & 50	09:47-15:13	142.2	49.8	0.0436
Run 3	50 & 100	09:20-16:03	247.3	46.6	0.0783
Run 4	16 & 33	10:10-15:43	265.7	44.3	0.0871
Run 5	50	10:31-16:07	359.0	45.1	0.157
Run 6	50 & 100	10:23-16:41	369.7	50.2	0.144
Reference bag	N/A	N/A	372.0	30.0	N/A

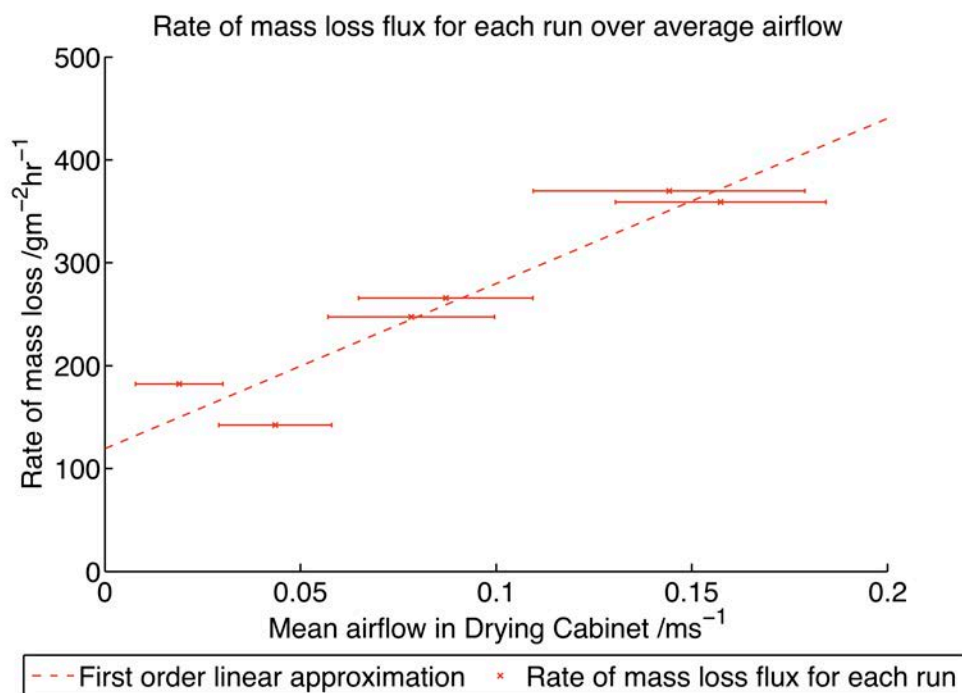


Fig. 5: Graphical representation of the drying flux versus air flow velocity from the values represented in Table 3 to identify the relationship between drying flux and flow rate. The points in Figure 5 and 6 are from corresponding runs.

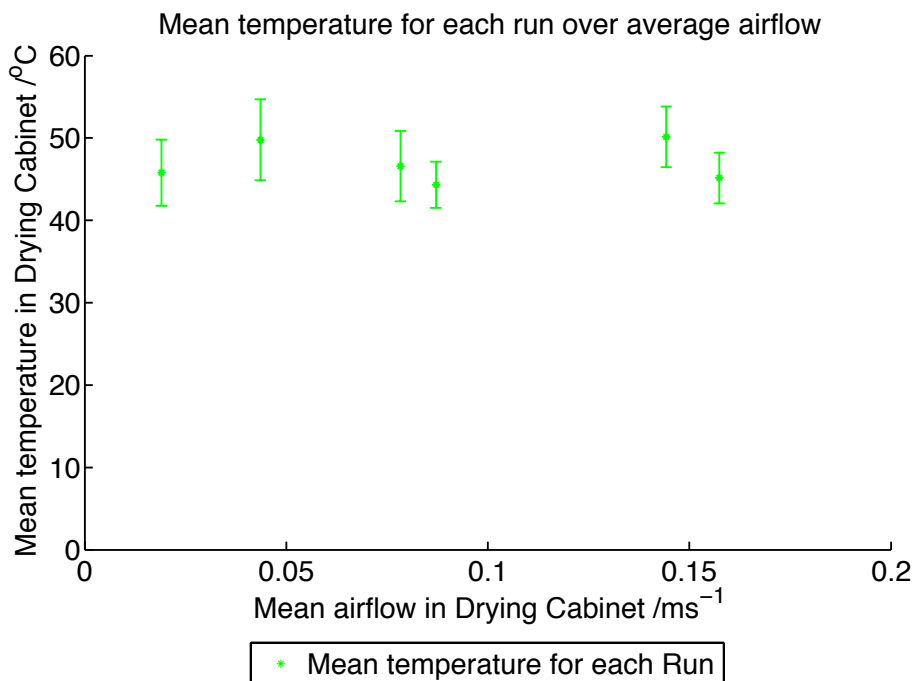


Fig. 6: Graphical representation of the temperature versus air flow velocity from the values represented in Table 3. The points in Figure 5 and 6 correspond, and with a small variation in temperature, a clear relationship between drying flux and flow rate is identified.

5. Measurement Uncertainties

Measurements with the hand anemometer to measure the air flow rate in the collector had complications due to fluctuating values with random variations in intervals. The fluctuation was affected by external wind which can create regions of turbulence and affect the measurements. The anemometer can only operate in laminar regions (Operation and Service Manual, Model 8330 VELOCICHECK 1994). The air flows measured in the collector were low, and small variations in wind led to large relative errors.

6. Discussion & Conclusion

6.1. Discussion

As can be seen in Table 3, the mass loss fluxes in the solar dryer never exceeded that of the reference bag. When this was discovered, during Runs 1 to Run 3, the driving forces of the drying process that differed between the dryer and ambient environment were analysed in order to identify the limiting factor on mass transport for the system. The temperature in the drying cabinet had increased by around 20 degrees compared to the ambient temperature, as seen in Table 3, and the relative humidity was lowered from 59.9 % (ambient) to 26.3 % (drying cabinet) on the 11th of May. This is one data point logged and the relation is similar during all performed tests. This corresponded with our predicted requirements for drying, but effectively it showed little effect. The most crucial parameters that differed between the drying cabinet and ambient environment were the direct sunlight on the reference bag in the sun and ambient wind passing over all reference bags. Direct sunlight was deemed to play a certain role in increasing the temperature of the reference bag. However, since it is transparent, it was not thought to have increased the temperature more than the 20

degrees which was the case in the drying cabinet. Ambient wind, or air flow passing over the bags, was thus investigated further.

The increased airflow velocity had a positive effect on the drying flux, as the drying flux was doubled between Run 1 and Run 6 which can be seen in Table 3 and Figure 5. If we relate the drying flux to eq. 1 in the Theory section, this suggests that the limiting factor for mass loss inside the drying cabinet was the mass transfer coefficient K , which is the only parameter dependent on airflow velocity. When the flow rate was actively increased in later test runs, the results showed an increase in drying flux. A hypothesis we suggest is that the limiting factor was not the diffusion of water through the membrane during the simulated “constant rate drying period” (i.e. when the drying flux is normally constant at the beginning of juice drying). If this was the case, an increased temperature would have led to an increased diffusion as it is driven by the difference in partial pressure as a function of relative humidity on the different sides of the membrane. However, the problem faced was not getting water to the surface of the membrane, but rather removing the already surfaced water.

6.2. Conclusion

Higher temperatures and a lower relative humidity inside the solar dryer did not increase the drying flux to the level of the reference bag placed in ambient conditions where passing wind and direct sunlight were available. A drying flux of $247.3 \text{ g}\cdot\text{m}^{-2}\cdot\text{h}^{-1}$ was reached during Run 3 compared to the drying flux of $372.0 \text{ g}\cdot\text{m}^{-2}\cdot\text{h}^{-1}$ for the reference bag. The solar dryer seemed to be missing the capacity to remove the vapour from the surface of the bag to continue the pervaporation process through the membrane. One hypothesis is that the air flow velocity was limiting the drying. A design modification, increasing the flow rate by 100%, by decreasing the volume of the drying cabinet doubled the drying flux between Runs 1 and Run 6, from $182.3 \text{ g}\cdot\text{m}^{-2}\cdot\text{h}^{-1}$ to a drying flux of $369.7 \text{ g}\cdot\text{m}^{-2}\cdot\text{h}^{-1}$. The hypothesis of air flow rate acting as an active parameter during the beginning stages of drying using Solar Assisted Pervaporation with membrane bags seems to be correct, but further research should be done to confirm this. It was concluded that the drying flux in the cabinet increased with the increased air flow rate due to a smaller cross section area, while temperature was maintained around the lower limit of the required temperature interval and a lower relative humidity than ambient was achieved.

7. Acknowledgements

We direct a large thank you to all sources of inspiration and help we have received during the project. We would like to send a special mention to Dr. Henrik Davidsson, Dr. Pia Otte and Dr. Lucas Tivana. Your academic guidance and practical knowledge have contributed greatly to the work. We also direct a thank you to our financiers, Åforsk, Kaptan Hanssons minnesfond, Bengt Ingeströms stipendiefond and the Espersen Foundation. It is with their generosity this project has been made possible.

8. References

- Cengel, Y. A., Boles, M. A., 2011. *Thermodynamics: An Engineering Approach*, seventh ed. McGraw-Hill.
- Ekechukwu, O.V., Norton, B., 1997. Review of solar-energy drying systems II: an overview of solar drying technology. *Energy Conversion and Management*. 40, 657-667.
- FAOSTAT, Food and Agriculture Organization of The United Nations Statistics Division, 2015. *Food Balance Mozambique*. Accessed on 07/03/2016. <http://faostat3.fao.org/compare/E>
- Bergman, T. L., Lavine, A. S., Incropera, F. P., DeWitt, D. P., 2007. *Fundamentals of Heat and Mass Transfer*, volume 1, sixth ed. Michigan: John Wiley.
- Johansson, P., Svensson, A., 1998. *Metoder för Mätning av Luftflöden i Ventilationsinstallationer*. Bygghälsningsrådet, Stockholm, Sweden.
- Néel J., 1991. Introduction to Pervaporation, in *Pervaporation membrane separation processes*, R.Y.M. Huang, Ed. Amsterdam: Elsevier, pp. 1-109
- Otte, P., 2014. Solar cooking in Mozambique an investigation of end-user's needs for the design of solar cookers. *Energy Policy*. 24, 366-375.
- Paul, S. 2013. *Introduction to Food Engineering*. Academic Press.
- Pervatech BV. 2014. *Pervaporation: An Overview Separation Technology Articles - Chemical Engineering - Frontpage - Cheresources.com*. Accessed on 18/03/2016. <http://www.cheresources.com/content/articles/separation-technology/pervaporation-an-overview?pg=1>
- Phinney, R., Rayner, M., Sjöholm, I., Tivana L., Dejmek P., 2015. *Solar Assisted Pervaporation (SAP) for Preserving and Utilizing Fruits in Development Countries.*, Third Southern African Solar Energy Conference, 11-13 May 2015.
- Rab A., Sajid, N, M., Bibi, F., Jan, I., Nabi, G., Najia, K., 2015. Quality changes in heat treated sweet orange fruit during storage a low temperature. *The Journal of Animal and Plant Sciences*. 25, 661-668.
- Saravacos G.D., and Kostaropoulos, A.E., 2002. *Handbook of Food Processing Equipment*, New York: Kluwer Academic/Plenum Publishers.
- TSI –Incorporated. 1994. *Operation and Service Manual, Model 8330 VELOCICHECK*

Appendix: NOMENCLATURE

Table A1: Nomenclature used in the report

Quantity	Symbol	Unit
Specific heat capacity	C_p	$\text{J kg}^{-1} \text{K}^{-1}$
Density	ρ	kg m^{-3}
Mass transfer rate	\dot{m}	kg s^{-1}
Global Irradiance	G	W m^{-2}
Mass transfer coefficient	K	$\text{kg/m}^{-2} \text{s}^{-1} \text{Pa}^{-1}$
Surface Area of bag	A_s	m^2
Collector Area	A_c	m^2
Relative Humidity	RH	%
Heat gained by collector	\dot{Q}_{gain}	W
Air flow rate	v	m s^{-1}
Inflow Temperature (collector)	T_{in}	$^{\circ}\text{C}$
Outflow Temperature (collector)	T_{out}	$^{\circ}\text{C}$
Thermal Efficiency	$\eta_{thermal}$	%
Partial pressure of water vapour on inside of the bag at surface temperature T_1	$p_{w,sat @ T_1}$	Pa
Partial pressure of water vapour on outside of bag at ambient temperature T_2	$p_{w,\infty @ T_2}$	Pa